3D Corneal Shape After Implantation of a Biosynthetic Corneal Stromal Substitute

Jeb A. Ong,[1,2] Edouard Auvinet,[3] Karolyn J. Forget,[1] Neil Lagali,[4] Per Fagerholm,[4] May Griffith,[1,4] Jean Meunier,[2,3] and Isabelle Brunette[1,2]

[1]Maisonneuve-Rosemont Hospital Research Center, Montreal, Quebec, Canada
[2]Department of Ophthalmology, University of Montreal, Montreal, Quebec, Canada
[3]Department of Computer Science and Operations Research, University of Montreal, Montreal, Quebec, Canada
[4]Integrative Regenerative Medicine Centre, Department of Clinical and Experimental Medicine, Linköping University, Linköping, Sweden

Correspondence: Isabelle Brunette, Department of Ophthalmology, Maisonneuve-Rosemont Hospital, 5415 boulevard de L'Assomption, Montreal, QC H1T 2M4 Canada; i.brunett@videotron.ca.

Submitted: September 25, 2015
Accepted: March 20, 2016

Citation: Ong JA, Auvinet E, Forget KJ, et al. 3D corneal shape after implantation of a biosynthetic corneal stromal substitute. *Invest Ophthalmol Vis Sci*. 2016;57:2355–2365. DOI:10.1167/iovs.15-18271

Purpose. The current and projected shortage of transplantable human donor corneas has prompted the development of long-term alternatives to human donor tissue for corneal replacement. The biosynthetic stromal substitutes (BSS) characterized herein represent a potentially safe alternative to donor organ transplantation for anterior corneal stromal diseases. The goal of this phase 1 safety study was to characterize the three-dimensional (3D) corneal shape of the first 10 human patients implanted with a BSS and assess its stability over time.

Methods. Ten patients underwent anterior lamellar keratoplasty using a biosynthetic corneal stromal implant for either advanced keratoconus or central corneal scarring. Surgeries were performed at Linköping University Hospital, between October and November 2007. Serial corneal topographies were performed on all eyes up to a 4-year follow-up when possible. Three-dimensional shape average maps were constructed for the 10 BSS corneas and for 10 healthy controls. Average 3D shape corneal elevation maps, difference maps, and statistics maps were generated.

Results. The biosynthetic stromal substitutes implants remained stably integrated into the host corneas over the 4-year follow-up period, without signs of wound dehiscence or implant extrusion. The biosynthetic stromal substitutes corneas showed steeper surface curvatures and were more irregular than the healthy controls.

Conclusions. Corneal astigmatism and surface steepness were observed 4 years after BSS implantation, while the implants remained stably integrated in the host corneas. Future studies will indicate if biomaterials technology will allow for the optimization of postoperative surface irregularity after anterior stromal replacement, a new window of opportunity that is not available with traditional corneal transplantation techniques.

Keywords: corneal implants, artificial cornea, corneal topography, corneal transplantation, keratoconus

Corneal blindness is the fourth leading cause of blindness worldwide. Despite the 100,000 transplantations performed every year, making the cornea one of the most commonly transplanted tissues,[1] prevalence of corneal blindness continues to rise, with around 2 million new cases per year.[2] Eye banks are unable to meet this demand and as a result, approximately 10 million patients are currently awaiting corneal transplantation.[3]

The rapidly evolving lamellar keratoplasty techniques seen of late has permitted to alleviate the exclusion criteria for tissue donation and increase the proportion of transplantable donor corneas, thus decreasing the waiting list for corneal transplantation. For instance, in Descemet's membrane endothelial keratoplasty (DMEK), only the endothelial and Descemet's membrane (DM) layers are transplanted, allowing eye banks to accept epithelial damage or stromal scars. Similarly, in deep anterior lamellar keratoplasty (DALK), only the corneal layers anterior to DM are transplanted. Descemet's membrane endothelial keratoplasty and DALK thus allow the safe use of donor corneas that would be rejected for penetrating keratoplasty (PK). Some surgeons have begun performing split-cornea transplantation, using the anterior (epithelium, Bowman layer, and stroma) and posterior (endothelium-Descemet membrane layer) portions for two different patients in the hope of reducing the need for donor tissue by 50%.[4] This practice remains uncommon. Keratoprostheses (KPros) also salvage a small portion of corneas otherwise deemed unusable, given that in these cases, the donor cornea only serves as structural support for the prosthesis. These surgical techniques, by themselves, however, will not resolve the current and projected issue of worldwide shortage of transplantable human donor corneas, and there remains an unmet need for long-term alternatives to human donor tissue.

The new concept of biosynthetic corneal substitute technology, whether partial or full thickness, represents a major breakthrough in the realm of corneal replacement. The

Investigative Ophthalmology & Visual Science

ideal corneal substitute would allow safe replacement of the diseased corneal layers, without risk of disease transmission from the donor or risk of immune rejection, and would allow for full rehabilitation of the corneal optical, biomechanical, and protective functions. It would also be affordable and commercially available in large numbers.

In 2010, Fagerholm et al.[5] published the first follow-up results of a phase I safety study where biosynthetic analogues of human corneal stromal matrices, comprising carbodiimide cross-linked recombinant human collagen (RHCIII, FibroGen, Inc., San Francisco, CA, USA), were implanted in the first 10 human patients by anterior lamellar keratoplasty. At 4 years post operation, the stromal implants remained stably integrated.[6] The use of recombinant human collagen avoids the risk of potential immune response[7,8] or disease transmission[9] associated with the transplantation of animal-source collagen. It was shown that by mimicking the extracellular matrix of the cornea, the biosynthetic implants promoted host tissue regeneration and repopulation by host epithelial cells, nerves, and keratocytes.[6,10,11] However, there has not been any detailed analysis of the shape of the implanted corneas. Tracking of corneal shape is important as it determines most of the eye's refractive power and hence, visual acuity.[12]

The goal of this study was to characterize the three-dimensional (3D) shape of the first human corneas implanted with biosynthetic stromal substitutes (BSS). The complementary methodologies used to achieve this goal included (1) the review of all individual topographies obtained before and after surgery for these 10 patients; (2) the creation of average topography maps to identify common shape patterns among the 10 implanted corneas; and (3) the construction of average difference maps to compare the implanted corneas at different time points. The three-dimensional shape of the implanted corneas was compared to that of normal corneas and (4) the analysis of standard shape parameters extracted from the individual topographies and giving a more traditional description of the 3D corneal shape. Finally, comparative data from the literature describing currently accepted corneal transplantation methods were analyzed.

Methods

Patients

The research protocol adhered to the tenets of the Declaration of Helsinki and it was approved by the Swedish Medical Products Agency and the Regional Ethical Review Board in Linköping, Sweden (application no. M205-06), trial registration (EudraCT no. 2006-006585-42). All patients signed an informed consent after the nature and potential risks of the procedure were explained. Eight male and two female patients, aged 18 to 75 years, were grafted with corneal implants. In nine cases, surgery was warranted by advanced keratoconus and in one case by corneal scarring impinging on the visual axis. A mean (± SD) follow-up of 3.52 ± 1.03 years was available at the time of this study. Only 3-year follow-up topographies were available for patients 1 and 9, and a 1-year topography for patient 4. For each patient, a control topography from a healthy subject was used. These controls were matched for age and sex and had a spherical equivalent within ± 3.00 D from emmetropia and a refractive cylinder of less than 1.00 D.

Surgery

All surgeries consisted of anterior lamellar keratoplasties performed by one of us (P.F.) between October and November 2007 at the Linköping University Hospital, Sweden. Only one eye per patient underwent surgery. The anterior diseased portion of the cornea was manually removed to a depth of 400 μm and on a diameter ranging from 6.0 to 6.5 mm, leaving only a thin layer of posterior stroma, DM, and endothelium. The 500 μm-thick, highly transparent corneal implant was trephined using a circular punch 0.25 mm larger in diameter than the recipient bed. It was then anchored into the recipient bed with three to four overlying 10-0 nylon mattress sutures, as shown in Figure 1. All sutures were removed during the same visit, on average 6.5 ± 3 weeks after surgery.

Average Map Construction

All topography maps reported in this paper consisted of corneal elevation maps. Elevation maps were favored over curvature maps because they provide more comprehensive shape information, subsequently allowing for any type of derived analysis, including calculation of curvatures. An average map has the same appearance as an individual map, the only difference being that each color point on the average map represents the average at this specific point of all the individual measurements for the studied population. The average map construction methodology used in this study has been described elsewhere.[13] Essentially, average anterior surface elevation maps were built from individual anterior surface topographies obtained with the Orbscan II system (Orbscan, Bausch & Lomb, Rochester, NY, USA) and saved into numerical tables of 101 by 101 points uniformly spaced and centered on the visual axis. Left eye topographies were horizontally flipped to convert them into right eyes (enantiomorphism).[14] Prior to averaging, spatial alignment of individual corneas was performed. Each individual topography Best-Fit Sphere (BFS) was aligned with a reference BFS, herein defined as the mean BFS of all healthy controls. The Best-Fit Sphere represents the sphere that best adjusts to the corneal surface with least-squares regression. In order to facilitate interpretation, the color scale used for the average elevation maps was the same as that commonly used in the commercial topography system for individual topographies (5-μm color steps, green representing a point on the BFS).

Difference Maps

A first difference map was used to compare the corneas before and after surgery. It was computed so that each color point represented the average of all paired differences at this specific point. A P value map complemented the difference map, highlighting in red areas of significant difference ($P < 0.05$) and in green, areas of insignificant difference ($P \geq 0.05$).[13,15] In order to assess shape stability of the corneas implanted with the BSS, herein called the BSS corneas, a second difference map was similarly generated comparing the earliest follow-up data (within the 1- to 2-year postoperative interval) to the latest follow-up data (within the 3- to 4-year postoperative interval). Exact time points of postoperative topographies used to calculate this difference map are listed in Supplementary Figure S1 and no replicate measurements were used for any of the average or difference maps. A third difference map was generated to compare the preoperative diseased corneas with the healthy controls ($n = 10$). And finally, a fourth difference map was generated to compare the 10 corneas implanted with the BSS at the time of their last visit to the healthy controls. These last two difference maps were expressed by computing a point-by-point difference between the two groups' average maps.

Investigative Ophthalmology & Visual Science

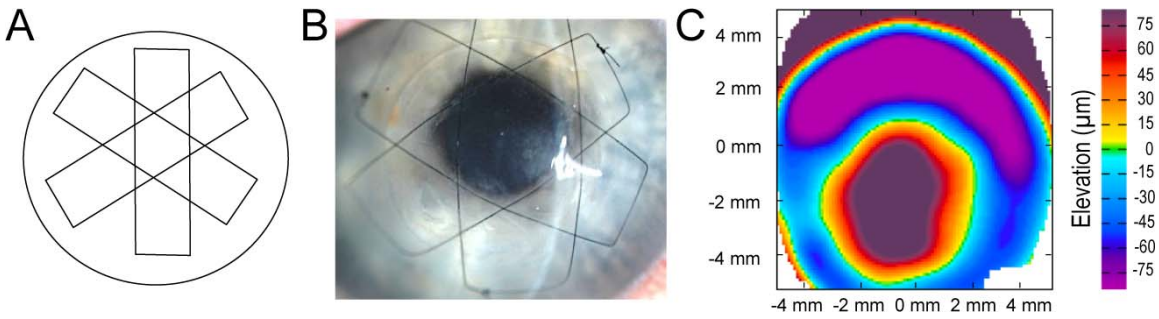

FIGURE 1. Hexagonal pattern of the mattress sutures imprinted on the anterior corneal surface of the BSS implant (patient #4). (**A**) Diagram of the mattress sutures placement. (**B**) Slit-lamp photograph of the cornea showing the mattress sutures over the BSS implant. (**C**) Corneal topography.

Standard Corneal Shape Parameters

Several topography parameters commonly used to characterize the corneal shape were also studied, including asphericity, apical radius of curvature, corneal power, astigmatism, and surface irregularity. The corneal asphericity coefficient (Q) indicates the rate at which the corneal curvature changes from the center to the periphery. In a perfect sphere, $Q = 0$. A Q value < 0 indicates that the corneal surface curvature gradually flattens from center to periphery (prolate shape). A Q value $>$ 0 indicates that the corneal curvature gradually steepens from center to periphery (oblate). The apical radius of curvature (R) characterizes the circle tangent to the apex (point of greatest curvature). The smaller the R value, the greater the curvature is, and vice versa. The mean corneal power (Mean Pwr) and astigmatism (Astig Pwr) were measured in the central 0- to 3-mm radius zone and in the 3- to 5-mm annular peripheral zone. Astigmatism (Astig) in the 1.5-mm radius central zone was reported as the difference between the Maximum (Max K) and Minimum (Min K) keratometry values, respectively, describing curvature in the steepest and flattest axes. Orientation of the astigmatism was classified as with-the-rule (steep axis within $\pm$ 22.5° from vertical), against-the-rule (steep axis within $\pm$ 22.5° from horizontal), or oblique (steep axis within $\pm$ 22.5° from either the 45° or 135° oblique axes). Surface irregularity was assessed using the Surface irregularity index given by the Orbscan system.

Statistical Analyses

Mean values and standard deviations are reported. Student's *t*-tests were used to test for differences in means between groups and for the point-by-point comparisons of the topography maps, with adjustment of *P* values according to Benjamini's correction for multiple comparisons.[16] Two-tailed paired Student's *t*-tests were used to compare pre- and postoperative values within the BSS group and two-tailed unpaired Student's *t*-tests were used to compare the BSS corneas to the healthy controls. The Pearson product-moment correlation coefficient was calculated to assess correlations between parameters. The Fisher exact test was used to test for homogeneity. A *P* value of less than 0.05 was considered to be statistically significant. All statistical tests were two-sided. The analyses were conducted using SAS 9.2 (SAS Institute, Inc., Cary, NC, USA) for the shape parameters and Matlab R2011A (Mathworks, Natick, MA, USA) for average maps comparisons.

RESULTS

Individual pre- and postoperative topographies are shown in Figures 2A, 2B, and Supplementary Figure S1. Average elevation maps and corresponding standard deviation maps are illustrated in Figure 3A, and difference maps with corresponding *P* value maps are illustrated in Figure 3B.

Healthy Corneas

The healthy subjects' average corneal elevation map shown in Figure 3A (column 1, top row) displayed the concentric pattern typical of healthy corneas. The apex, in warm colors (i.e., above the BFS), was surrounded by cold colors (under the BFS), themselves surrounded by another ring of increasingly warmer colors toward the periphery. Variability among healthy individuals was low ($\pm$ 1.8–8.1 µm in the 3-mm radius central area), as shown by the yellow and green standard deviation map (Fig. 3A, column 1, second row).

Corneal Shape Before BSS Implantation

The individual preoperative topographies were available for all patients except one (patient #5; Fig. 2A). The nine keratoconus corneas had the typical shape of keratoconic eyes (#1–#9), with a pronounced paracentral prominence surrounded by a ring of relative depression below the BFS.

This pattern is well summarized by the preoperative average map shown in Figure 3A, column 2. Standard deviation in the diseased eyes before BSS implantation was much larger ($\pm$ 9–48 µm in the 3-mm radius central area) than that seen in the healthy controls. The diseased corneas before BSS implantation were statistically significantly different from the healthy corneas, as shown by the difference map and the predominantly red *P* value map (Fig. 3B, column 1).

Corneal Shape After BSS Implantation

Figure 2B shows the postoperative topographies at the time of the last visit for the 10 BSS corneas. The biosynthetic stromal substitutes implants appeared to be well integrated into the host corneas. There were no signs of wound dehiscence or implant extrusion, as evidenced by the absence of gaps, steps, or extreme changes in curvature at the level of the wound.

The biosynthetic stromal substitutes corneas were appreciably more irregular than the healthy controls. Two patterns predominated. (1) A localized, central, or paracentral prominence (Fig. 2B) was most notable in patients #3, 4, and 7. This prominence tended to adopt a hexagonal contour, which matched the area delineated by the overlying mattress sutures (Figs. 1A–C). (2) A tendency in flattening of the superior cornea was also noted, which was most distinct in patients #3, 4, and 5, but also seen in patients #1, 7, 9, and 10 (Fig. 2B). These observations were well illustrated by the postoperative average map (Fig. 3A, column 3), showing a paracentral, hexagonal elevation (in orange) and a superior

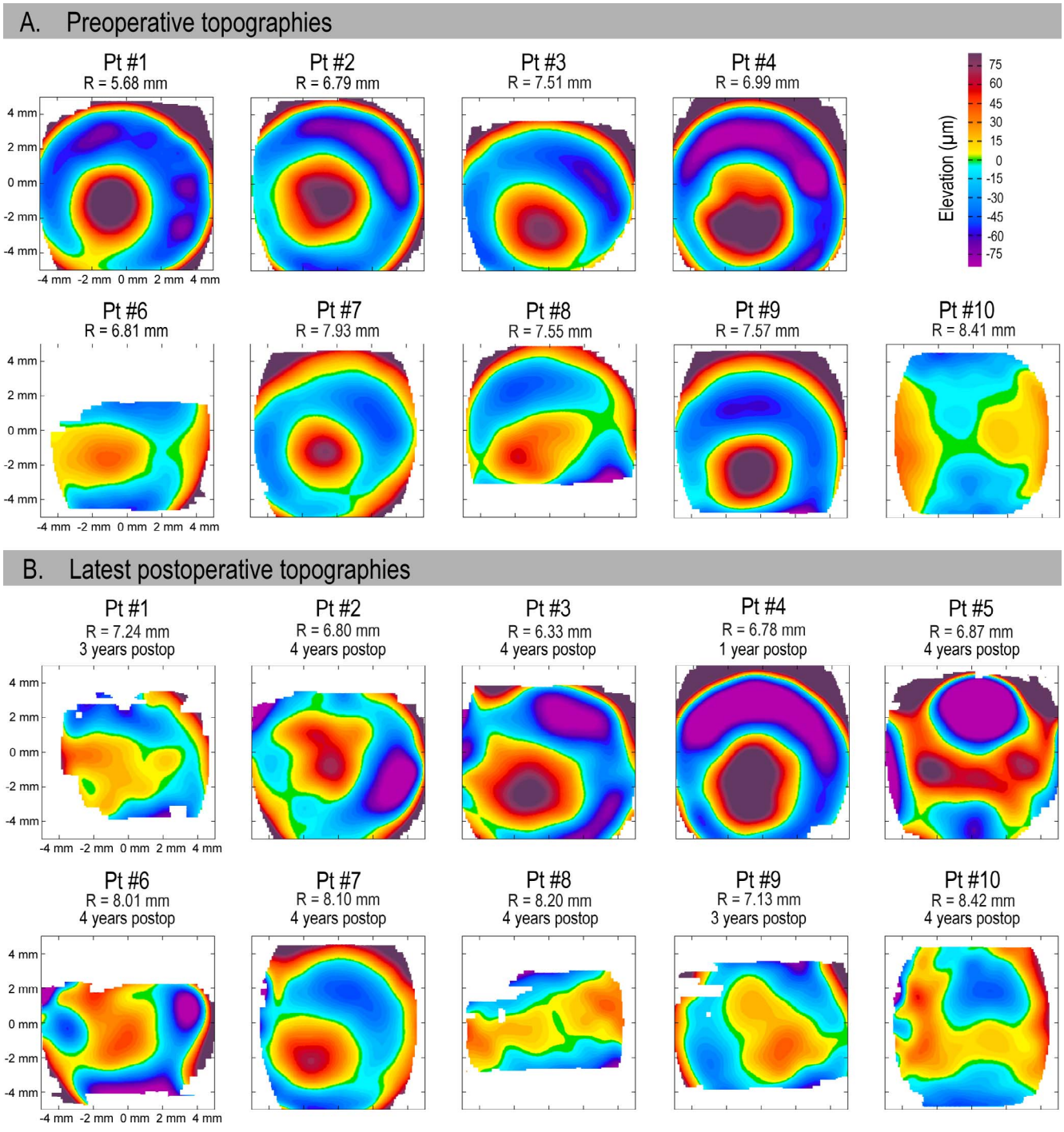

Figure 2. Individual topographies of the 10 BSS patients. (**A**) Preoperative topographies. (**B**) Postoperative topographies taken at the time of the last visit.

crescent-shaped flattening (in purple-blue). The standard deviation map confirmed the variability among postoperative corneas (± 11–66 µm in the 3-mm radius central area).

The overall effect of BSS implantation is summarized by the mean difference map obtained by subtracting the preoperative topographies from the postoperative topographies (Fig. 3B, column 2), and consisted essentially in a flattening of the cone (central blue area). The amount of flattening varied between patients and did not reach statistical significance, as shown by the almost entirely green *P* value map (Fig. 3B, column 2, second row).

Comparison of the postoperative BSS corneas to healthy controls (Fig. 3B, column 3) confirmed the presence of a hexagonal, paracentral bulging and a flattening of the superior cornea at the level of the superior lid in the operated eyes.

Standard Corneal Topography Parameters

Standard corneal topography parameters, including asphericity, apical radius of curvature, corneal steepness, astigmatism, and surface irregularity, were also studied before and after surgery

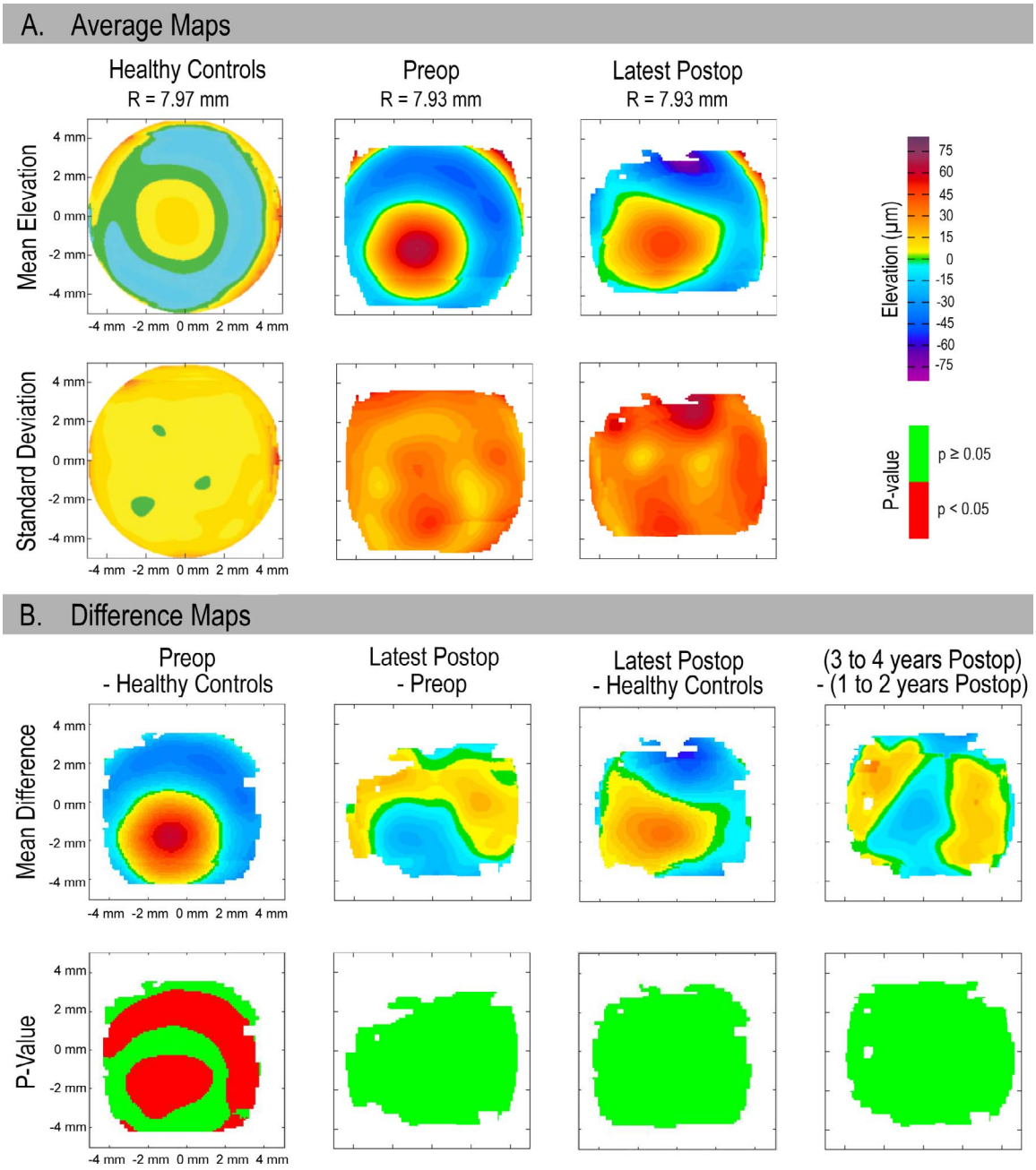

Figure 3. Average topography maps. (**A**) Average elevation maps. *First row*: Average elevation maps; *Second row*: Standard deviation maps. *Column 1*: Healthy controls maps (average model of 10 healthy controls matched for age and sex). *Column 2*: Preoperative maps (average of preoperative topographies). *Column 3*: Postoperative maps (average of latest postoperative topographies). (**B**) Difference maps. *First row*: Difference maps; *Second row*: *P* value maps. *Column 1*: Preoperative—Healthy controls difference map (difference between the healthy controls and the preoperative average maps). *Column 2*: Latest postoperative—Preoperative difference map (average map of the paired differences between the preoperative and the latest postoperative topographies). *Column 3*: Latest postoperative—Healthy controls difference map (difference between the healthy controls average map and the latest postoperative average map). *Column 4*: (3- to 4-year postoperative) – (1- to 2-year postoperative) difference map (average map of the paired differences between the earliest topography taken between the first and second years and the latest topography taken between the third and fourth years after implantation). Time points for each of the postoperative topographies used to build these difference maps are detailed in Supplementary Figure S1.

(Table 1; Figs. 4A–F). Comparisons between pre- and postoperative values showed a mild flattening and decrease in the amount of surface irregularity in the 0- to 3-mm central cornea. These changes, however, did not reach statistical significance (Table 1). Astigmatism in the 0- to 1.5-mm area also showed a mild improvement, while it increased in the more peripheral zones. Surface irregularity increased in the 3- to 5-mm surgical wound zone.

Comparisons between BSS implanted corneas and the healthy controls showed the following: No significant difference in asphericity (Q) was found between the two groups (Table 1) and the corneal power (Mean Pwr) values of the BSS corneas overlapped those of the healthy eyes (Fig. 4A). Corneal power, corneal astigmatism, and their variability, were statistically significantly higher in the BSS corneas than in healthy eyes, both in the central and peripheral zones (Table 1;

Table 1. Comparison of BSS and Normal Subjects

	BSS Preoperative, Mean ± SD	BSS Postoperative, Mean ± SD	Controls, Mean ± SD
Number of subjects	10	10	10
Age	43.0 ± 19.1	46.7 ± 19.0	47.6 ± 18.2
Shape parameters			
R	6.99 ± 0.87*	6.84 ± 1.01†	7.74 ± 0.14
Q	−0.20 ± 0.62	−0.26 ± 0.56	−0.13 ± 0.20
0- to 1.5-mm central zone			
Max K (KD)	54.49 ± 8.71*	52.08 ± 6.52†	43.75 ± 0.96
Min K (KD)	47.84 ± 7.13	46.03 ± 7.32	43.04 ± 0.82
Astig (KD)	6.64 ± 2.89*	6.05 ± 2.49†	0.71 ± 0.43
0- to 3-mm central zone			
Surface irregularity (KD)	8.85 ± 3.11*	8.81 ± 3.45†	1.25 ± 0.55
Mean Pwr (KD)	49.43 ± 6.06*	49.23 ± 5.75†	43.45 ± 0.73
Astig Pwr (KD)	3.82 ± 2.17*	5.46 ± 5.48†	0.98 ± 0.78
3- to 5-mm peripheral zone			
Surface irregularity (KD)	10.24 ± 3.79*	11.71 ± 5.19†	1.61 ± 0.46
Mean Pwr (KD)	46.91 ± 4.34*	47.49 ± 4.84†	43.06 ± 0.81
Astig Pwr (KD)	2.35 ± 1.29*	3.65 ± 2.32†	0.63 ± 0.27

* The comparison of the BSS corneas before surgery and the normal controls was statistically significant (Student's unpaired *t*-test; $P < 0.05$).
† The comparison between the BSS-implanted corneas and the normal controls was statistically significant (Student's unpaired *t*-test; $P < 0.05$). The differences between BSS corneas before and after surgery did not reach statistical significance.

Figs. 4B–D). Surface irregularity was also significantly higher in BSS eyes, especially at the level of the surgical wound and sutures (Fig. 4E). The preferential with-the-rule orientation of astigmatism, typically preponderant among healthy eyes and observed herein in healthy controls (steep axis close to vertical in 64% of cases), was also observed in the BSS eyes (Fig. 4F). In summary, the BSS corneas were steeper and more irregular than the healthy controls. Their overall asphericity, however, was not significantly different from that of healthy eyes.

Visual Acuity, Corneal Shape, and Refraction

Before surgery, the best spectacle corrected visual acuity (BSCVA) was counting fingers in two patients and the average BSCVA for the rest was 0.74 logMAR (ranging from 0.5 to 1 logMAR).[5] At 4 years post implantation, the average BSCVA for the 10 patients was 0.88 logMAR (0.4–1.0 logMAR).[6] While all patients who received the biosynthetic implants were contact lens-intolerant before surgery, most of them tolerated rigid contact lenses after surgery. When considering contact-lens corrected scores (BCLVA), the mean visual acuity at 4 years was 0.44 logMAR (0.1–1 logMAR), meaning that it improved from preoperative values in eight patients (mean gain of 0.56 logMAR units, ranging from 0.3 to 1.7 logMAR) and remained unchanged in two. Figures 5A through 5C describe the evolution of visual acuity throughout the study period. Overall, visual acuity was shown to improve continuously from before to 1 to 2 years after BSS implantation ($P = 0.0054$) and from 1 to 2 years to 3 to 4 years after BSS implantation ($P = 0.0126$).

While no correlations were found between the BSCVA in logMAR and spherical equivalent refraction (Fig. 5D) or refractive cylinder (Fig. 5E), statistically significant positive correlations were found between the BSCVA in logMAR and corneal power (Fig. 5F) and surface irregularity (Fig. 5G). A significant negative correlation was also found between the BSCVA and the apical radius of curvature (Fig. 5H). In other words, visual acuity was better when the implanted corneas were less steep, less irregular, and closer to the shape of the healthy controls (Figs. 5F–I). In addition, the keratometric parameters (power and surface irregularity) were better indicators of spectacle corrected visual acuity than the strength of the spectacle (amount of refractive spherical equivalent and cylinder; Figs. 5D–I).

Stability of BSS Implanted Corneas Over Time

In order to assess the overall stability in time of the BSS corneas, a map was produced consisting of the mean difference in 3D shape observed between the earliest (within the 1- to 2-years postoperative interval) and the latest (within the 3- to 4-years interval) follow-up visits (Fig. 3B, column 4). Time points of the postoperative topographies used to calculate this difference map are detailed in Supplementary Figure S1. The mild postoperative flattening of the central protrusion seen over time was not statistically significant (*P*-value map entirely green).

Discussion

The clinical concept of implanting a corneal substitute instead of an ex vivo native cornea is new and represents the endpoint to many years of development.[6,10,11,17] As reported recently, these recombinant human collagen anterior stromal implants promote rapid re-epithelialization, as well as colonization by the recipient's keratocytes and nerves, allowing for the rehabilitation of corneal function.[5,6] Results of this safety study showed that these implants were stably integrated into the host corneas, without signs of wound dehiscence or implant extrusion. Because of the small sample size of this phase I safety study and because of the variation observed among the individuals, several analyses were underpowered and did not reach statistical significance. Trends in data, however, were observed: the surgery induced a mild flattening of the corneas. The analyses also revealed postoperative irregular astigmatism, the presence of a hexagonal, central prominence delineated by the overlying mattress suture pattern, and a flattening of the superior cornea under the superior lid. Average maps were more informative about shape distribution across the corneal surface than were corneal shape parameters, which only focused on specific aspects of the shape and were more likely affected by focal irregularities.

Investigative Ophthalmology & Visual Science

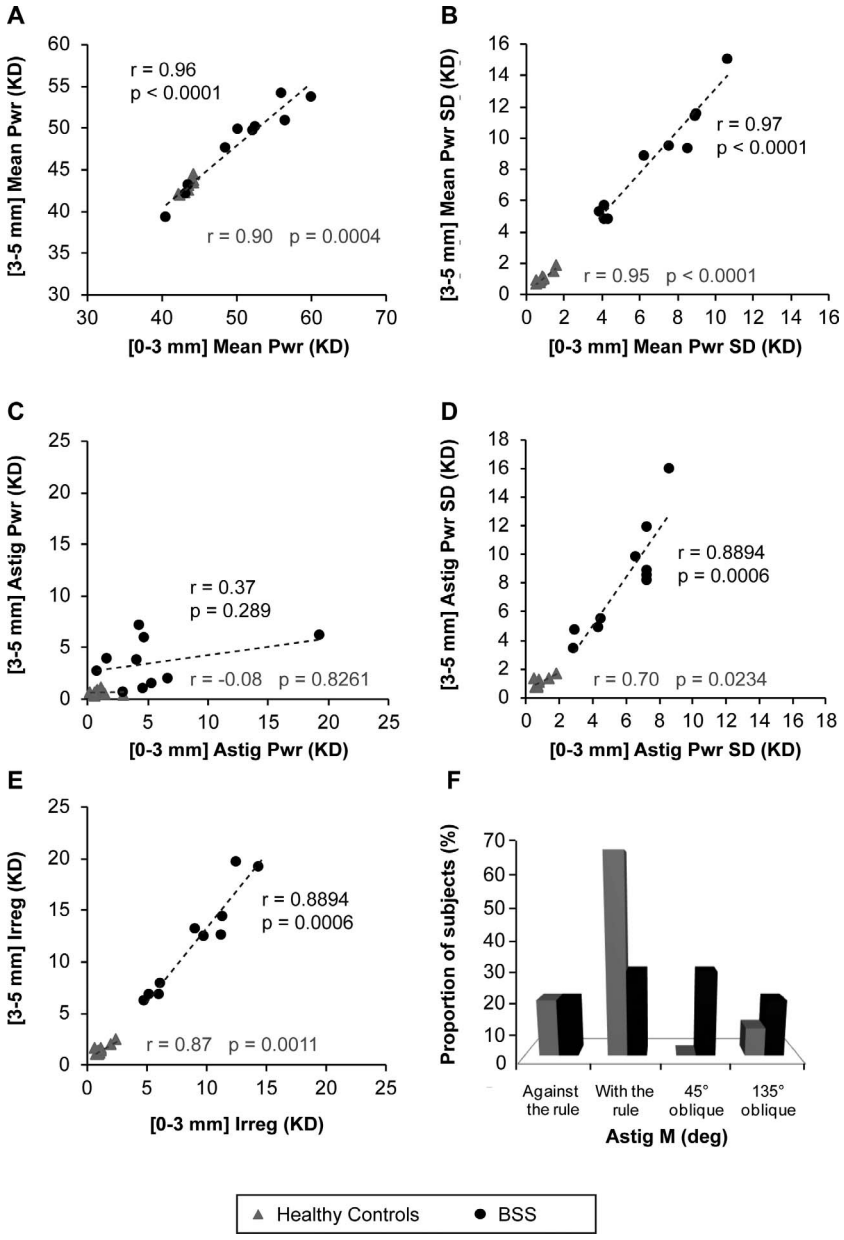

Figure 4. Distribution of the corneal shape parameters for BSS implanted and healthy control eyes. (**A**) Mean power as a function of corneal zone. (**B**) Mean power standard deviation as a function of corneal zone. (**C**) Astigmatism as a function of corneal zone. (**D**) Astigmatism standard deviation as a function of corneal zone. (**E**) Surface irregularity as a function of corneal zone. (**F**) Orientation of corneal astigmatism.

Comparison of BSS Implantation With Traditional Corneal Transplantation

Until recently, the only widely accepted surgical options for the replacement of corneas with end-stage keratoconus or anterior stromal scars were PK and DALK, using eye bank donor corneas. Table 2 compares the corneal shape parameter values reported in the literature after PK or DALK with those reported herein after BSS implantation. Neither PK, DALK, nor BSS have been reported to yield corneal topography values similar to those observed in normal nonoperated eyes.

Comparison With Penetrating Keratoplasty

Penetrating keratoplasty, which consists in the replacement of the full thickness of the cornea, remains the gold standard for corneal transplantation. Despite generally good postoperative corrected visual acuity,[18–22] PK often leaves significant ametropia and severe astigmatism, and most importantly, these results are unpredictable. Mean astigmatism values of 3.4 to 4.9 D, ranging from 0.5 to 8.98 D are typically reported after PK.[18,20,23,24] Our results show that the BSS corneas were steeper (49.23 ± 5.75 D) than usually described after PK (43.00–45.9; Table 2).[18,22,24] Corneal astigmatism in BSS eyes was also higher than routinely reported after PK, with a mean value of 6.05. Surface irregularity of BSS corneas was approximately double that reported in post-PK patients.[20]

Comparison With Deep Anterior Lamellar Keratoplasty

In deep anterior lamellar keratoplasty, the full thickness of the diseased stroma is replaced, preserving only the host's 20-μm

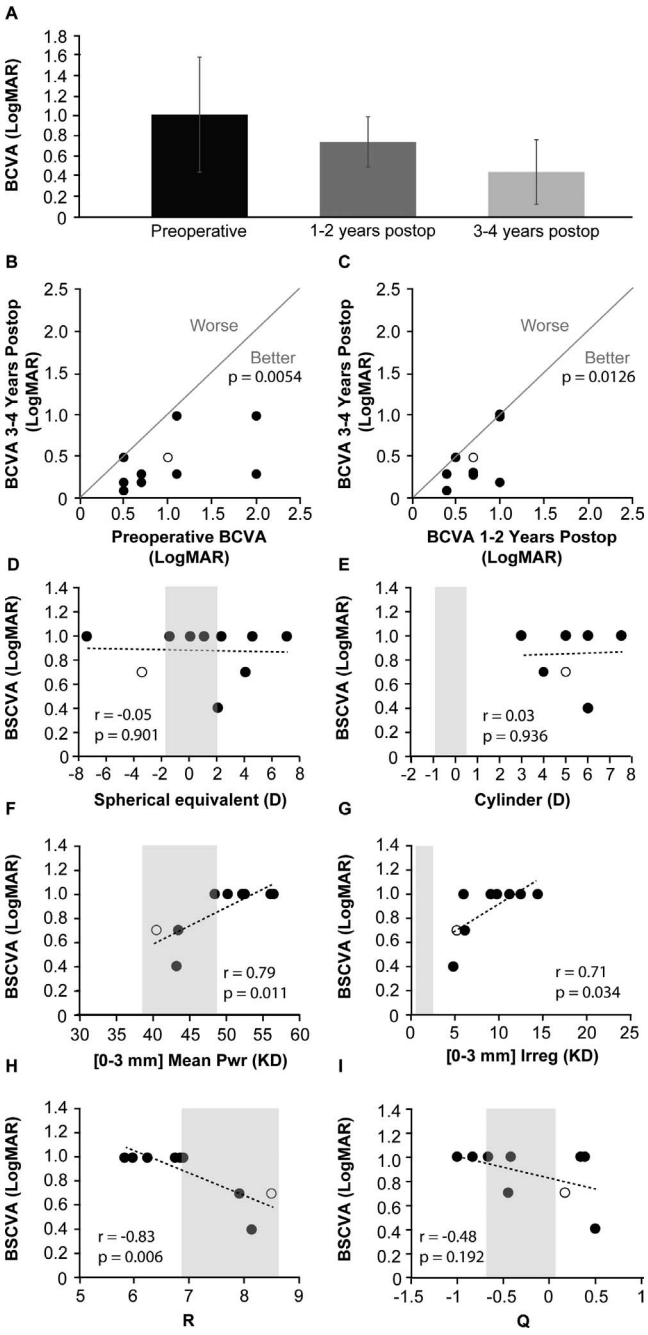

Figure 5. Visual acuity progression and correlation with shape parameters. (**A**) Evolution of best corrected visual acuity (BCVA) over time. (**B**) Evolution of BCVA from before to 1 to 2 years after BSS implantation. (**C**) Evolution of BCVA from 1 to 2 years to 3 to 4 years after BSS implantation. Correlations between BSCVA and (**D**) spherical equivalent refraction, (**E**) refractive cylinder, (**F**) mean power, (**G**) surface irregularity in the central 0- to 3-mm radius zone, (**H**) apical radius of curvature (R), and (**I**) asphericity (Q) for eyes implanted with a BSS at the time of the latest postoperative visit. Visual acuity is reported in logMAR units (0 logMAR = 20/20 and 1 logMAR = 20/200). *Zones in grey* represent the range of values measured in healthy controls. *Empty circles* represent the patient with corneal scar.

thick endothelial and Descemet's layers.[23] As far as the global 3D corneal shape is concerned, the outcome after DALK is thus very similar to that after PK, with residual steepness, a large range of astigmatism, and surface irregularity.[25] Our results showed that central corneal steepness after BSS implantation was more than that reported for DALK (44.4–47.2 D), DALK and PK both inducing more flattening than BSS in keratoconus eyes.[22,26–28] However, peripheral corneal steepness in BSS eyes was comparable to that found in the literature for DALK (47.84 ± 5.37 D; Table 2).[24] The mean astigmatism value for the BSS corneas was higher than those for DALK (2.25–5.41 D)[20,23,24,26–29] and surface irregularity was approximately double that reported post-DALK.[20]

Ten of the 12 articles cited in Table 2 included only keratoconus patients, one mainly involved keratoconus patients and in the other, keratoconus patients showed results similar to those of their entire study group, thus allowing us to compare these historical results to those of the BSS patients. In addition, complete suture removal had been performed by the time final measurements were taken in all studies cited, as it was the case for the BSS implants. One notable point is that the BSS corneas tolerated a relatively short suture removal time of 6.5 ± 3 weeks after surgery. Sutures are rarely removed until 1 year after PK and between 5 and 27 months after DALK.[26] As sutures can lead to several complications, including infection, vascularization, and rejection, and knowing that late suture removal delays visual rehabilitation, earlier removal, when possible, represents an advantage.

Visual Acuity and Corneal Shape

Visual acuity improved continuously throughout the study period ($P < 0.05$). Visual acuity was shown to be closely linked to corneal shape and surface irregularity. The increased corneal steepness, the irregular astigmatism due to the overlying mattress sutures, and the corneal flattening under the superior lid have all, to some extent, affected visual acuity in the BSS implanted eyes. The small size of the implants (6.25–6.75 mm diameter) also induced irregular astigmatism, as confirmed by the mean surface irregularity index in the 3- to 5-mm wound zone. Larger graft diameters ranging from 7.50 to 8.75 mm are generally used for DALK and PK, to minimize surface distortion due to the wound and sutures[30,31] and postoperative myopia.[32] This is especially important for keratoconus eyes, for which corneal ectasia often extends far into the residual host peripheral cornea.[25,31] It should be noted that the stromal haze described previously at the stromal-implant interface[5] most probably also affected visual acuities.[23] A deep anterior lamellar keratoplasty surgical technique using larger graft diameter implants will be considered for future clinical trials.

Traditional Limits of Corneal Replacement Using Human Native Tissue

At the present time, only DMEK allows restitution of an almost perfectly normal corneal shape after corneal lamellar transplantation, with practically optimal visual rehabilitation.[33,34] All transplantation techniques involving a corneal surface wound and sutures to hold the graft (whether the graft is anterior lamellar, deep anterior lamellar, or full thickness) potentially induce significant astigmatism, ametropia (usually on the myopic side), and surface irregularity, with a large variability in the results (Table 2).[35–40] Postoperative corneal shape is influenced by the inevitable disparities in curvature and thickness between the donor and recipient corneas, as well as by the architecture of the donor and recipient cuts. Various attempts have been made to optimize corneal shape-related outcomes following PK or DALK. Mechanical and femtosecond laser assisted trephination techniques have been refined to ensure better apposition between donor and host corneas,[21,41–44] and great attention has been paid to the recipient bed and graft diameters,[31,45] as well as to suturing techniques.[29,46,47] A number of refractive surgery procedures

Table 2. Postoperative Topography Parameters for BSS, PK, DALK, and Normal Subjects

	BSS	PK	DALK	Normal
Q[12,18,48-57]	−0.26 ± 0.56	−0.14		−0.18 to −0.36
0- to 1.5-mm central zone				
Astig[18,20,23,24,26–29,36–38,58,59]	6.05 ± 2.49	3.4 to 4.9	2.25 to 5.41	0.8 to 1.0
Maximum K[28,35–39,60]	52.08 ± 6.52		45.53 to 47.52	43.81 to 44.87
Minimum K[35–39,60]	46.03 ± 7.32		43.8	42.82 to 43.92
0- to 3-mm central zone				
Mean Pwr[18,24,35,36,59,61]	49.23 ± 5.75	43.0 to 45.9	44.4 to 47.2	43.29 to 49.3
Astig Pwr[35,36]	5.46 ± 5.48			1.13 to 1.22
Surface irregularity[20,36,38,40]	8.81 ± 3.45	3.31 ± 1.2	3.0 ± 0.7	1.05 to 1.25
3- to 5-mm peripheral zone				
Mean Pwr[24,36]	47.49 ± 4.84	45.03 ± 4.65	47.84 ± 5.37	48.78 ± 1.68
Astig Pwr[36]	3.65 ± 2.32			0.94 ± 0.44
Surface irregularity[20,36,38,40]	11.71 ± 5.19	5.88 ± 1.6	5.32 ± 1.2	1.73 to 2.05

All keratometric units in Diopters; Q and surface irregularity index have no units. Data are expressed as the mean, and when only one study is reported, standard deviation is also mentioned.

have also been developed to improve corneal shape in postkeratoplasty eyes, including relaxing incisions, intracorneal ring segments, and topography guided photoablative surgery. Despite major efforts, however, surface irregularity and instability remain a challenge with traditional PK or DALK techniques.

Potential of Biosynthetic Corneal Implants

Based on the analysis reported herein and based on the literature, BSS implantation, which is still at its earliest stages, faces the same limitations as traditional transplantation techniques in terms of 3D corneal shape, namely astigmatism, steepness, and surface irregularity. Although BSS have not proven to be superior with regards to 3D shape outcomes, the adjustments needed to exceed the standard methods of transplantation are theoretically accessible. Given that astigmatism, steepness, and surface irregularity are outcomes related to the biomechanical properties of the implant's material and that the latter can be optimized during production, biomaterials technology may offer an entirely new window of opportunity. The rigid poly (methyl methacrylate) (PMMA) used to produce KPros represents an example of stable surface shape control in the context of corneal replacement. Poly (methyl methacrylate), however, contrary to recombinant human collagen biomaterials, is an inert material, incompatible with colonization by host's cells and corneal tissue regeneration. Further studies are needed to confirm that increasing the BSS biomaterial's rigidity will allow sutures to be placed more peripherally, with less suture imprinting, resulting in smoother re-epithelialization. Future studies will also indicate if more rigid biosynthetic material can better mask the central keratoconic protrusion and better resist compression by the upper eyelid. In this context, comparing the 3D shape of BSS implanted corneas with that of healthy corneas becomes particularly interesting, as it allows to better understand and guide the future development of biosynthetic implants.

In conclusion, previous studies have shown that the recombinant human collagen stromal implants offer significant advantages over native transplants, including sterility and absence of immune rejection. They represent a potentially safe alternative to donor organ transplantation for anterior stromal disease, with active colonization by the recipient's epithelial cells, keratocytes, and nerves. The present study focused on the 3D corneal shape of the first 10 human patients implanted with a BSS. It showed that these implants remained stably integrated into the host corneas over the 4-year follow-up period, without signs of wound dehiscence or implant extrusion. The biosynthetic stromal substitutes corneas showed steeper surface curvatures and were more irregular than the healthy controls. Future studies will show if optimization of implant biomaterial properties will help minimize postoperative astigmatism and ametropia, an opportunity that is not available for traditional corneal transplantation techniques using human donor tissue.

Acknowledgments

The authors thank Kimberley Merrett who optimized the BSS implants; as well as Marie-Eve Choronzey, BA, Georges Durr, MD, Marina Gilca, MD, Marie-Claude Perron, MSc, Élodie Samson, MSc, and Fatma Zaguia for their technical and/or intellectual support.

Presented in part at the annual meeting of the Association for Research in Vision and Ophthalmology, Fort Lauderdale, Florida, United States, May 2012 (Preliminary results).

Supported by Canadian Institutes of Health Research MOP 106517 (IB) and Stem Cell Network (MG), Ottawa, ON, Canada; FRQS Research in Vision Network, Montreal, QC, Canada (IB); County Council of Östergötland, Sweden (PF). IB is the recipient of the Charles-Albert Poissant Research Chair in Corneal Transplantation, University of Montreal, Canada. Funding organizations had no role in the design or conduct of this research. The authors have no proprietary or commercial interest in any materials discussed in this article. A patent submission related to the biomaterials formulation described in this study was assigned to the Ottawa Hospital Research Institute, Ottawa, ON, Canada, and is currently licensed to Eyegenix, Inc., a wholly-owned subsidiary of Cellular Bioengineering, Inc. (CBI), Hawaii for use in the field of corneal transplantation. None of the authors have any links to Eyegenix or CBI. The authors alone are responsible for the content and writing of the paper.

Disclosure: **J.A. Ong**, None; **E. Auvinet**, None; **K.J. Forget**, None; **N. Lagali**, None; **P. Fagerholm**, None; **M. Griffith**, None; **J. Meunier**, None; **I. Brunette**, None

References

1. Tan D. World Sight Day: Singapore's contribution to alleviating corneal blindness. *Ann Acad Med Singapore*. 2012;41:427–429.

2. Poisson J. How to fix the cornea transplant system. Available at: http://www.thestar.com/news/gta/2011/07/20/how_to_fix_the_cornea_transplant_system.html. Accessed December 19, 2013.
3. Acuité. Des malvoyants recouvrent la vue grâce à une cornée artificielle en collagène. Available at: http://www.acuite.fr/articles.asp?REF=6385. Accessed December 19, 2013.
4. Heindl LM, Riss S, Laaser K, Bachmann BO, Kruse FE, Cursiefen C. Split cornea transplantation for 2 recipients - review of the first 100 consecutive patients. *Am J Ophthalmol*. 2011;152:523–532.
5. Fagerholm P, Lagali NS, Merrett K, et al. A biosynthetic alternative to human donor tissue for inducing corneal regeneration: 24-month follow-up of a phase 1 clinical study. *Sci Transl Med*. 2010;2:46ra61.
6. Fagerholm P, Lagali NS, Ong JA, et al. Stable corneal regeneration four years after implantation of a cell-free recombinant human collagen scaffold. *Biomaterials*. 2014;35:2420–2427.
7. Liu L, Kuffova L, Griffith M, et al. Immunological responses in mice to full-thickness corneal grafts engineered from porcine collagen. *Biomaterials*. 2007;28:3807–3814.
8. Lynn AK, Yannas IV, Bonfield W. Antigenicity and immunogenicity of collagen. *J Biomed Mater Res B Appl Biomater*. 2004;71:343–354.
9. Manuelidis EE, Angelo JN, Gorgacz EJ, Kim JH, Manuelidis L. Experimental creutzfeldt-jakob disease transmitted via the eye with infected cornea. *N Engl J Med*. 1977;296:1334–1336.
10. Liu Y, Gan L, Carlsson DJ, et al. A simple, cross-linked collagen tissue substitute for corneal implantation. *Invest Ophthalmol Vis Sci*. 2006;47:1869–1875.
11. Merrett K, Fagerholm P, McLaughlin CR, et al. Tissue-engineered recombinant human collagen-based corneal substitutes for implantation: performance of type I versus type III collagen. *Invest Ophthalmol Vis Sci*. 2008;49:3887–3894.
12. Gatinel D. *Topographie cornéenne*. Paris: Elsevier Masson; 2011:172.
13. Laliberte JF, Meunier J, Chagnon M, Kieffer JC, Brunette I. Construction of a 3-D atlas of corneal shape. *Invest Ophthalmol Vis Sci*. 2007;48:1072–1078.
14. Durr GM, Auvinet E, Ong J, Meunier J, Brunette I. Corneal shape, volume, and interocular symmetry: parameters to optimize the design of biosynthetic corneal substitutes. *Invest Ophthalmol Vis Sci*. 2015;56:4275–4282.
15. Brunette I, Sherknies D, Terry MA, Chagnon M, Bourges JL, Meunier J. 3-D characterization of the corneal shape in Fuchs dystrophy and pseudophakic keratopathy. *Invest Ophthalmol Vis Sci*. 2011;52:206–214.
16. Benjamini Y, Hochberg Y. Controlling the false discovery rate: a practical and powerful approach to multiple testing. *J R Statist Soc Ser B*. 1995;57:289–300.
17. Li F, Carlsson D, Lohmann C, et al. Cellular and nerve regeneration within a biosynthetic extracellular matrix for corneal transplantation. *Proc Natl Acad Sci U S A*. 2003;100:15346–15351.
18. Langenbucher A, Seitz B, Naumann GO. Three-axis ellipsoidal fitting of videokeratoscopic height data after penetrating keratoplasty. *Curr Eye Res*. 2002;24:422–429.
19. Demers PE, Steinert RF, Gould EM. Topographic analysis of corneal regularity after penetrating keratoplasty. *Cornea*. 2002;21:140–147.
20. Javadi MA, Feizi S, Yazdani S, Mirbabaee F. Deep anterior lamellar keratoplasty versus penetrating keratoplasty for keratoconus: a clinical trial. *Cornea*. 2010;29:365–371.
21. Chamberlain WD, Rush SW, Mathers WD, Cabezas M, Fraunfelder FW. Comparison of femtosecond laser-assisted keratoplasty versus conventional penetrating keratoplasty. *Ophthalmology*. 2011;118:486–491.
22. Javadi MA, Motlagh BF, Jafarinasab MR, et al. Outcomes of penetrating keratoplasty in keratoconus. *Cornea*. 2005;24:941–946.
23. Ardjomand N, Hau S, McAlister JC, et al. Quality of vision and graft thickness in deep anterior lamellar and penetrating corneal allografts. *Am J Ophthalmol*. 2007;143:228–235.
24. Kim KH, Choi SH, Ahn K, Chung ES, Chung TY. Comparison of refractive changes after deep anterior lamellar keratoplasty and penetrating keratoplasty for keratoconus. *Jpn J Ophthalmol*. 2011;55:93–97.
25. Reinhart WJ, Musch DC, Jacobs DS, Lee WB, Kaufman SC, Shtein RM. Deep anterior lamellar keratoplasty as an alternative to penetrating keratoplasty a report by the American Academy of Ophthalmology. *Ophthalmology*. 2011;118:209–218.
26. Feizi S, Javadi MA, Jamali H, Mirbabaee F. Deep anterior lamellar keratoplasty in patients with keratoconus: big-bubble technique. *Cornea*. 2010;29:177–182.
27. Fournie P, Coullet J, Moalic S, Malecaze F, Chapotot E, Arne JL. Deep anterior lamellar keratoplasty in the surgical treatment of keratoconus. A 1-year follow-up. *J Fr Ophtalmol*. 2006;29:602–613.
28. Kubaloglu A, Sari ES, Unal M, et al. Long-term results of deep anterior lamellar keratoplasty for the treatment of keratoconus. *Am J Ophthalmol*. 2011;151:760–767.
29. Acar BT, Vural ET, Acar S. Does the type of suturing technique used affect astigmatism after deep anterior lamellar keratoplasty in keratoconus patients? *Clin Ophthalmol*. 2011;5:425–428.
30. Krachmer JH, Mannis MJ, Holland EJ. *Cornea*. Philadelphia: Elsevier Mosby; 2005.
31. Skeens HM, Holland EJ. Large-diameter penetrating keratoplasty: indications and outcomes. *Cornea*. 2010;29:296–301.
32. Jensen AD, Maumenee AE. Refractive errors following keratoplasty. *Trans Am Ophthalmol Soc*. 1974;72:123–131.
33. Goldich Y, Showail M, Avni-Zauberman N, et al. Contralateral eye comparison of descemet membrane endothelial keratoplasty and descemet stripping automated endothelial keratoplasty. *Am J Ophthalmol*. 2015;159:155–159.
34. Hamzaoglu EC, Straiko MD, Mayko ZM, Sales CS, Terry MA. The first 100 eyes of standardized descemet stripping automated endothelial keratoplasty versus standardized descemet membrane endothelial keratoplasty. *Ophthalmology*. 2015;122:2193–2199.
35. Pinero DP, Alio JL, Aleson A, Escaf Vergara M, Miranda M. Corneal volume, pachymetry, and correlation of anterior and posterior corneal shape in subclinical and different stages of clinical keratoconus. *J Cataract Refract Surg*. 2010;36:814–825.
36. Liu Z, Huang AJ, Pflugfelder SC. Evaluation of corneal thickness and topography in normal eyes using the Orbscan corneal topography system. *Br J Ophthalmol*. 1999;83:774–778.
37. Tananuvat N, Pansatiankul N. Assessment of the anterior structures of eyes in a normal Northern Thai group using the Orbscan II. *J Med Assoc Thai*. 2005;88(suppl 9):S105–S113.
38. KhabazKhoob M, Hashemi H, Yazdani K, Mehravaran S, Yekta A, Fotouhi A. Keratometry measurements, corneal astigmatism and irregularity in a normal population: the Tehran Eye Study. *Ophthalmic Physiol Opt*. 2010;30:800–805.
39. Fam HB, Lim KL. Corneal elevation indices in normal and keratoconic eyes. *J Cataract Refract Surg*. 2006;32:1281–1287.
40. Lim L, Wei RH, Chan WK, Tan DT. Evaluation of keratoconus in Asians: role of Orbscan II and Tomey TMS-2 corneal topography. *Am J Ophthalmol*. 2007;143:390–400.

Investigative Ophthalmology & Visual Science

41. Moshirfar M, Calvo CM, Kinard KI, Williams LB, Sikder S, Neuffer MC. Comparison of Hanna and Hessburg-Barron trephine and punch systems using histological, anterior segment optical coherence tomography, and elliptical curve fitting models. *Clin Ophthalmol*. 2011;5:1121–1125.
42. Seitz B, Langenbucher A, Naumann G. The penetrating keratoplasty. A 100-year success story. *Ophthalmologe*. 2005;102:1128–1139.
43. Por YM, Cheng JY, Parthasarathy A, Mehta JS, Tan DT. Outcomes of femtosecond laser-assisted penetrating keratoplasty. *Am J Ophthalmol*. 2008;145:772–774.
44. Bahar I, Kaiserman I, McAllum P, Rootman D. Femtosecond laser-assisted penetrating keratoplasty: stability evaluation of different wound configurations. *Cornea*. 2008;27:209–211.
45. Jaycock PD, Jones MN, Males J, et al. Outcomes of same-sizing versus oversizing donor trephines in keratoconic patients undergoing first penetrating keratoplasty. *Ophthalmology*. 2008;115:268–275.
46. Busin M, Monks T, al-Nawaiseh I. Different suturing techniques variously affect the regularity of postkeratoplasty astigmatism. *Ophthalmology*. 1998;105:1200–1205.
47. Feizi S, Javadi MA. Corneal graft curvature change after relaxing incisions for post-penetrating keratoplasty astigmatism. *Cornea*. 2012;31:1023–1027.
48. Read SA, Collins MJ, Carney LG, Franklin RJ. The topography of the central and peripheral cornea. *Invest Ophthalmol Vis Sci*. 2006;47:1404–1415.
49. Eghbali F, Yeung KK, Maloney RK. Topographic determination of corneal asphericity and its lack of effect on the refractive outcome of radial keratotomy. *Am J Ophthalmol*. 1995;119:275–280.
50. Horner DG, Soni PS, Vyas N, Himebaugh NL. Longitudinal changes in corneal asphericity in myopia. *Optom Vis Sci*. 2000;77:198–203.
51. Guillon M, Lydon DP, Wilson C. Corneal topography: a clinical model. *Ophthalmic Physiol Opt*. 1986;6:47–56.
52. Carney LG, Mainstone JC, Henderson BA. Corneal topography and myopia. A cross-sectional study. *Invest Ophthalmol Vis Sci*. 1997;38:311–320.
53. Kiely PM, Smith G, Carney LG. Meridional variations of corneal shape. *Am J Optom Physiol Opt*. 1984;61:619–626.
54. Zhang Z, Wang J, Niu W, et al. Corneal asphericity and its related factors in 1052 Chinese subjects. *Optom Vis Sci*. 2011;88:1232–1239.
55. Montalban R, Pinero DP, Javaloy J, Alio JL. Scheimpflug photography-based clinical characterization of the correlation of the corneal shape between the anterior and posterior corneal surfaces in the normal human eye. *J Cataract Refract Surg*. 2012;38:1925–1933.
56. Liu Y, Wang Y, Wang Z, Zuo T. Effects of error in radius of curvature on the corneal power measurement before and after laser refractive surgery for myopia. *Ophthalmic Physiol Opt*. 2012;32:355–361.
57. Douthwaite WA, Hough T, Edwards K, Notay H. The EyeSys videokeratoscopic assessment of apical radius and p-value in the normal human cornea. *Ophthalmic Physiol Opt*. 1999;19:467–474.
58. Dubbelman M, Sicam VA, Van der Heijde GL. The shape of the anterior and posterior surface of the aging human cornea. *Vision Res*. 2006;46:993–1001.
59. Huang T, Hu Y, Gui M, Hou C, Zhang H. Comparison of refractive outcomes in three corneal transplantation techniques for keratoconus. *Graefes Arch Clin Exp Ophthalmol*. 2015;253:1947–1953.
60. Arora R, Jain P, Jain P, Manudhane A, Goyal J. Results of deep anterior lamellar keratoplasty for advanced keratoconus in children less than 18 years. *Am J Ophthalmol*. 2016;162:191–198.
61. Romano V, Iovieno A, Parente G, Soldani AM, Fontana L. Long-term clinical outcomes of deep anterior lamellar keratoplasty in patients with keratoconus. *Am J Ophthalmol*. 2015;159:505–511.

Investigative Ophthalmology & Visual Science